

Gen4D: Synthesizing Humans and Scenes in the Wild

Jerrin Bright^{1,3}, Zhibo Wang^{1,3}, Yuhao Chen^{1,3}, Sirisha Rambhatla^{2,3},
John Zelek^{1,3}, David Clausi^{1,3}

¹ Vision and Image Processing Lab

² Critical ML Lab

³ University of Waterloo, Canada

{jerrin.bright, zhibo.wang, yuhao.chen1, sirisha.rambhatla, jzelek}@uwaterloo.ca



Figure 1: **Overview of the SportPAL dataset generated using our proposed framework, Gen4D.** (a) Examples of diverse canonical avatars synthesized via diffusion-guided prompt modeling, illustrating variation in clothing, body shape, and appearance. (b) Final synthetic frames rasterized with motion-driven avatar animation and human pose-aware backgrounds, demonstrating realistic lighting, shadows, and foot-ground interaction.

Abstract

Lack of input data for in-the-wild activities often results in low performance across various computer vision tasks. This challenge is particularly pronounced in uncommon human-centric domains like sports, where real-world data collection is complex and impractical. While synthetic datasets offer a promising alternative, existing approaches typically suffer from limited diversity in human appearance,

motion, and scene composition due to their reliance on rigid asset libraries and hand-crafted rendering pipelines. To address this, we introduce **Gen4D**, a fully automated pipeline for generating diverse and photorealistic 4D human animations. **Gen4D** integrates expert-driven motion encoding, prompt-guided avatar generation using diffusion-based Gaussian splatting, and human-aware background synthesis to produce highly varied and lifelike human sequences. Based on **Gen4D**, we present SportPAL, a large-scale syn-

*thetic dataset spanning three sports— baseball, icehockey, and soccer. Together, **Gen4D** and SportPAL provide a scalable foundation for constructing synthetic datasets tailored to in-the-wild human-centric vision tasks, with no need for manual 3D modeling or scene design.*

1. Introduction

Data collection and annotation are critical for any computer vision task [6, 14, 40]. The quality and quantity of the collected data directly influence the accuracy and reliability of the trained models [38, 50, 14, 36]. However, the process of data collection and annotation can be challenging, especially in the context of human-centric tasks, where the complexity and dynamism of human postures, coupled with variations in appearance, make it difficult to capture the full range of relevant information [3].

Due to the aforementioned issue, synthetic data is becoming increasingly popular for its ease of acquisition and well-annotated nature [38, 50, 6, 11, 5]. However, current synthetic data fall short in several key aspects necessary for broad applicability. For example, most existing approaches [38, 50, 39] rely on a library of 3D assets [1, 34], predefined motions [2, 33, 42, 49], or constrained rendering pipelines [7, 18] that result in repetitive appearances, restricted visual diversity, and oversimplified motion dynamics. Additionally, manually constructing large-scale synthetic datasets with meaningful variation in body types, actions, viewpoints, clothing, and lighting remains a labor-intensive and inflexible process, making it difficult to scale to diverse domains like sports or outdoor activities. Table 1 provides a detailed summary of existing datasets (real, rendered, and composite) for human-centric vision tasks.

Given the limitations of existing datasets, we ask: *Can we fully automate the synthesis of lifelike human animation from motion to scene, without any manual 3D modeling?*

Our answer is **yes**. In this paper, we introduce **Gen4D**, a fully automated pipeline for synthesizing diverse, lifelike 4D human animation datasets, combining dynamic motion with photorealistic scene generation. **Gen4D** leverages Gaussian splatting and text-conditioned diffusion models to generate realistic human sequences directly from text prompts. Motion trajectories are obtained through an expert-driven motion modeling module that extracts pose data from publicly available internet videos. The framework supports scalable creation of synthetic datasets with controllable variations over body shape, clothing, motion type, camera viewpoint, and environment.

With **Gen4D**, we introduce SportPAL (Figure 1), a large-scale synthetic dataset spanning three sports— baseball, icehockey, and soccer. SportPAL includes 2D bounding boxes, 2D and 3D pose annotations, SMPLX-based human modeling parameters, segmentation masks, and action la-

bels. The dataset comprises over half a million frames of human animations covering a wide range of actions, camera viewpoints, lighting conditions, and subject appearances, tailored for sports scenarios. Experimentation on the SportPAL dataset demonstrates its potential for human-centric tasks. Additionally, we evaluate the cross-sport generalization ability of a pose estimator trained on our synthetic data.

Our contributions can be summarized as follows: (1) We propose **Gen4D**, a fully automated pipeline for generating lifelike human models with realistic animations and backgrounds. (2) Based on **Gen4D**, we introduce SportPAL, a large-scale synthetic dataset spanning three sports- baseball, icehockey, and soccer, with rich annotations specifically designed for human-centric vision tasks.

2. Related Work

2.1. Real Datasets

Real-world images are inherently diverse, complex, and abundant. Many existing 2D pose datasets, such as COCO [30] and LSP [25], rely on these real images and require manual annotation of 2D poses. These datasets are often limited by the subjectivity and potential inconsistencies of human annotators, who may provide annotations that are constrained to the 2D plane and lack 3D information [3].

While 2D pose annotation is relatively straightforward, the challenge of 3D HPE has necessitated different approaches due to the inherent ambiguity of the task [9]. To address this, researchers have relied primarily on two approaches: marker-based and markerless motion capture systems [53, 23, 35, 45, 28, 37]. Marker-based systems [23, 45, 48] offer accurate groundtruth but are limited by the number of subjects, clothing variations, and controlled environments. Marker-less systems [35, 22, 53, 24] provide greater flexibility in terms of subject variability and real-world scenarios, but often suffer from less accurate groundtruth compared to marker-based methods.

All existing datasets demonstrated limitations in terms of complexity, pose diversity, and the accuracy of groundtruth data [23, 35, 45]. **Gen4D** addresses these challenges by leveraging text prompts and publicly available internet videos to generate a wide range of diverse and complex human-centric datasets.

2.2. Synthetic Datasets

Computer graphics has the potential to synthesize large-scale image datasets, where groundtruth is generated by animating human models such as SMPL [32] or GHUM [52]. PanopTOP [19] is a human-only synthetic dataset aimed at solving the distribution gap in real datasets that encompass a majority of frontal views. SURREAL [50] was one of the first works to open-source large-scale synthetic datasets for many different human-centric tasks, including 2D/3D pose

| Dataset | Environment | Subjects | Keypoints | Poses | Cameras | Markerless | FPS | Frames |
|------------------------|----------------|----------|-----------|-------|---------|------------|--------|--------|
| Human3.6M [23] | lab | 11 | 26 | 900K | 4 | × | 50 | 3.6M |
| MPI-INF-3DHP [35] | lab & outdoor | 8 | 28 | 93K | 14 | ✓ | 25/50 | 1.3M |
| 3DPW [51] | lab & outdoor | 7 | 24 | 49K | 1 | × | 30 | 51K |
| HumanEva-I [45] | lab | 6 | 15 | 78K | 7 | × | 60 | 280K |
| HumanEva-II [45] | lab | 6 | 15 | 3K | 4 | × | 60 | 10K |
| TotalCapture [48] | lab | 5 | 25 | 179K | 8 | × | 60 | 1.9M |
| CMU Panoptic [49] | lab | 8 | 18 | 1.5M | 31 | ✓ | 30 | 46.5M |
| AIST++ [28] | lab | 30 | 17 | 1.1M | 9 | ✓ | 60 | 10.1M |
| ASPset-510 [37] | outdoor | 17 | 17 | 110K | 3 | ✓ | 50 | 330K |
| SportsPose [22] | lab & outdoor | 24 | 17 | 177K | 7 | ✓ | 90 | 1.5M |
| WorldPose [24] | soccer pitch | - | 24 | 2.5M | - | ✓ | 50 | 150K |
| AthletePose3D [53] | lab & ice rink | 8 | 55/86 | 165K | 4/8/12 | ✓ | 60/120 | 1.3M |
| HSPACE [5] | rendered | 100 | GHUM [52] | 5M | 5 | ✓ | 60/120 | 1M |
| GTA-Human [11] | game | >600 | 24 | 1.4M | - | ✓ | N/A | 1.4M |
| 3DPeople [39] | composite | 80 | 3D joints | 2.5M | 4 | ✓ | N/A | 2.5M |
| AGORA [38] | rendered | >350 | 24/ 55 | 173K | 1 | ✓ | N/A | 18K |
| BEDLAM [6] | rendered | 217 | 55 | - | - | ✓ | N/A | 380K |
| SportPAL (ours) | synthetic | 50 | 55 | 583K | 18 | ✓ | N/A | 583K |

Table 1: Comparison of the SportPAL dataset with other datasets for human-centric vision tasks.

estimation, depth estimation, optical flow, and segmentation masks. Similarly, AGORA [38] proposes a synthetic dataset with high realism and highly accurate groundtruth. They aim to solve the generalizability issue by including person-person occlusions, environmental occlusions, crowds, and children’s data as part of their synthetic dataset.

Although the above works were promising, they were used in addition to real datasets to get the best performance. BEDLAM [6] was the first work that demonstrated that neural networks trained on synthetic data can achieve state-of-the-art accuracy in 3D human pose and shape estimation.

While these works mark promise, most of these datasets are constrained by the motion source obtained primarily from AMASS [33], CEASER [42], or CMU MoCap [49] datasets. Similarly, they tend to use a database of skin tones, hair, motion sequences, and clothing modeled using software like Blender [7] or Unreal Engine [18]. This limits their *applicability to in-the-wild dynamic scenarios*, which often require complex motion with varying body types, clothing, and environments. Thus, in contrast, our work **Gen4D** is a fully automated text-guided 4D human animation system, through which we create SportPAL — a large-scale, diverse, and realistic synthetic dataset tailored for in-the-wild human activities.

3. Method

In this section, we describe our end-to-end pipeline for generating motion-driven, photorealistic human avatars in diverse environments. Our method begins by extracting 3D motion data from real video demonstrations, capturing real-

istic body dynamics. We then generate a wide range of human avatars with varying appearances using prompt-driven diffusion-guided optimization. These avatars are then animated with the extracted motion, rendered from multiple camera viewpoints, and composited into realistic backgrounds that match the human pose context. This results in high-quality, fully synthetic human sequences suitable for training and evaluating vision models. An overview of the pipeline is shown in Figure 2.

3.1. Motion Extraction

Given a set of expert video demonstrations from publicly available internet videos, we utilize a pretrained human mesh recovery method [10] to extract the SMPLX [32] pose and shape parameters of the expert. Since each demonstration features a single focal expert, we normalize the shape parameters across the sequence. Following prior works [15, 8, 26], we regress these parameters to 3D joint coordinates using a predefined regression matrix $G \in \mathbb{R}^{K \times M}$, where K and M represent the number of joints and SMPL mesh vertices, respectively. The resulting 3D joints are then projected onto the image plane to obtain the 2D joint coordinates. We specifically opt for expert demonstrations to encode motion representations, rather than relying on language-driven models [47, 4, 44], as these models often fail to generate diverse and realistic motion sequences for complex, in-the-wild actions [43].

An important characteristic to note is that the accuracy of the extracted motion from the mesh recovery method [10] doesn’t need to perfectly match the observed pose of the person in the original video. Since our pipeline uses the es-

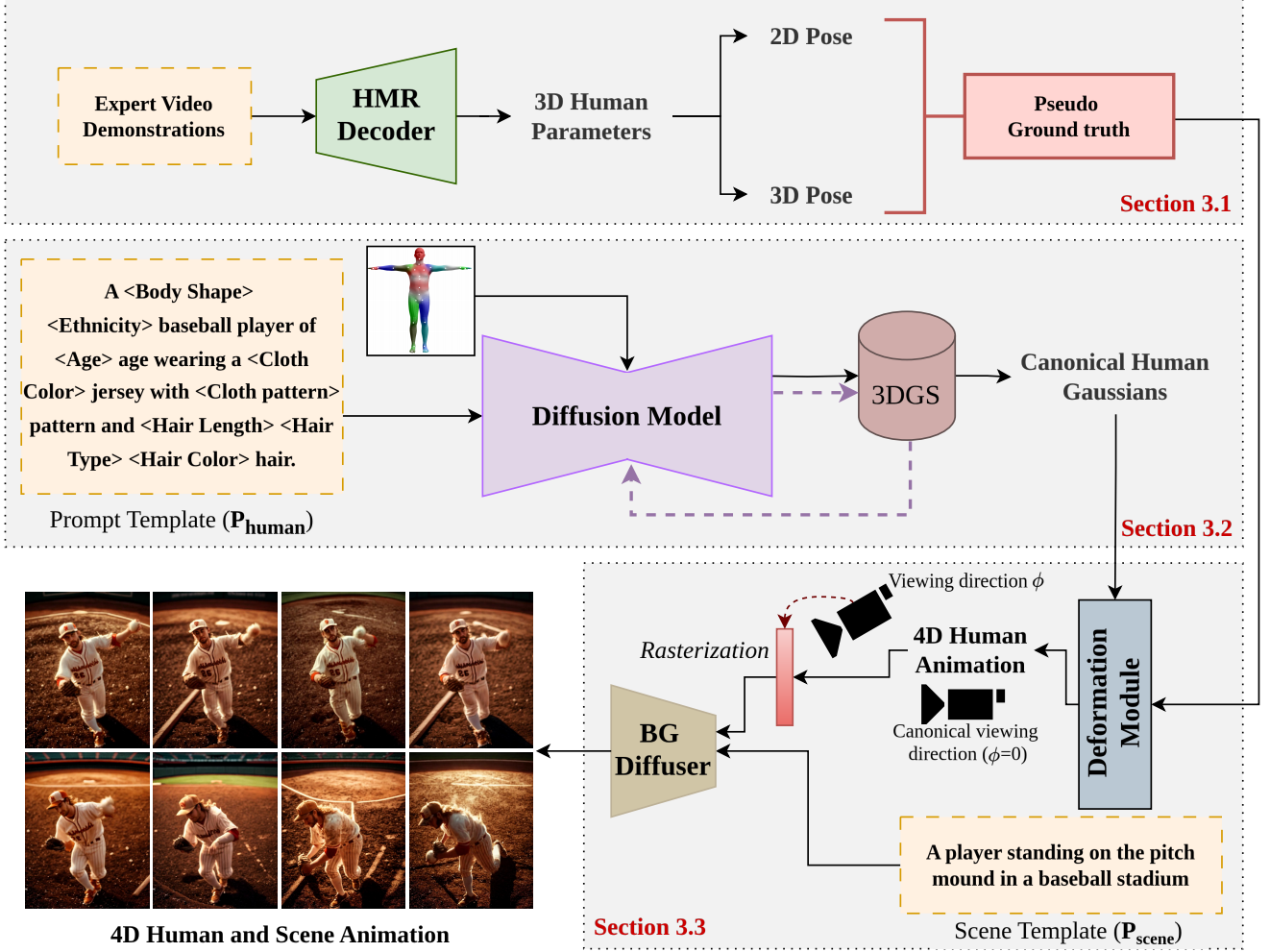


Figure 2: **The pipeline of Gen4D.** Our method consists of three stages: **Section 3.1 Motion Extraction** extracts 3D human motion from expert demonstrations; **Section 3.2 Canonical Human Gaussians** generates diverse human avatars via diffusion-guided Gaussian optimization; and **Section 3.3 Scene Composition** deforms avatars with motion, rasterizes them from varied viewpoints, and synthesizes realistic backgrounds using a scene-conditioned diffuser.

timated pose as the pseudo-motion to drive synthetic avatar animation (i.e., independent of the original viewpoint), we will still be able to generate perfect image–pose pairs in entirely new camera configurations for the corresponding rendered synthetic image.

3.2. Canonical Human Gaussians

Most prior works [21, 41, 20] use images or 3D scans to guide the initialized Gaussians towards realistic human representations. This limits the diversification of the model to the available visual data given as input. Thus, in this work, we optimize the Gaussian parameters using the synthesized RGB (x_c) and depth map (d_c) from a pretrained diffusion backbone [31] which is guided by text prompts. This approach is specifically chosen to introduce variability and flexibility in the generated human avatars.

Specifically, we first initialize a SMPLX human model in canonical space. Then we initialize the Gaussians on the canonical representation instead of initializing with random points or structure-from-motion (SfM) [46]. This ensures dense point distributions for initialization. Then, we utilize a pretrained diffusion model that is trained to simultaneously denoise RGB (x_c) and depth map (d_c) conditioned on a canonical 3D pose and prompt template (P_{human}).

Based on this, a dual-branch Score Distillation Sampling (SDS) [31] is used to optimize the human appearance and geometry of the initialized canonical representation. The loss can be computed as shown in Equation (1).

Attributes:

| | | | | | | | | |
|----------------|----------|----------|----------|------------|---------|---------|-----------|---------|
| Ethnicity: | American | Asian | African | Indian | ... | Mexican | → African | Fill in |
| Body Shape: | Slim | Athletic | Muscular | Fat | → Slim | | | Fill in |
| Age: | Teenager | Mid-aged | Old | → Teenager | | | Fill in | |
| Cloth Color: | Black | Red | White | Yellow | ... | Teal | → Yellow | Fill in |
| Cloth Pattern: | Solid | Stripes | Checks | Floral | ... | Dots | → Checks | Fill in |
| Hair Color: | Black | Brown | Red | Grey | ... | Bronze | → Grey | Fill in |
| Hair Type: | Straight | Curly | Wavy | Kinky | → Curly | | | Fill in |
| Hair Length: | Short | Medium | Long | → Medium | | | Fill in | |

Prompt Template:

A **Body Shape**
Ethnicity baseball
 player of **Age** age
 wearing a **Cloth Color**
 jersey with **Cloth**
 pattern pattern and
Hair Length **Hair Type**
Hair Color hair.

Generated Avatar:

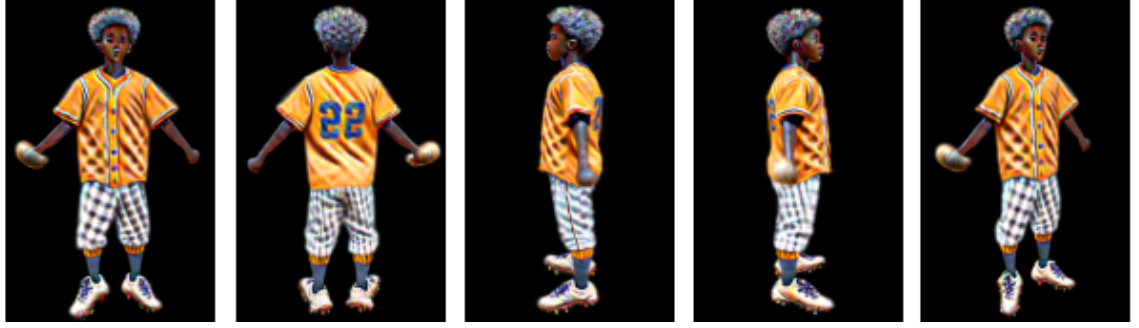


Figure 3: **Prompt modeling pipeline of Gen4D.** Diverse prompt templates are used to synthesize a variety of 3D canonical avatars, illustrated here from five different camera views.

$$\begin{aligned} \nabla_{\theta} \mathcal{L}_{\text{SDS}} = & \lambda_1 \cdot \mathbb{E}_{\epsilon_{\mathbf{x}_c}, t} \left[w_t (\epsilon_{\phi}(\mathbf{x}_c; p_c, \mathbf{P}_{\text{human}}) - \epsilon_{\mathbf{x}_c}) \frac{\partial \mathbf{x}_c}{\partial \theta} \right] \\ & + \lambda_2 \cdot \mathbb{E}_{\epsilon_{\mathbf{d}_c}, t} \left[w_t (\epsilon_{\phi}(\mathbf{d}_c; p_c, \mathbf{P}_{\text{human}}) - \epsilon_{\mathbf{d}_c}) \frac{\partial \mathbf{d}_c}{\partial \theta} \right] \end{aligned} \quad (1)$$

where λ_1 and λ_2 are coefficients that balance the effects between RGB and depth. We compute \mathcal{L}_{SDS} according to our parsed random render \mathcal{R}' for supervision. $\epsilon_{\phi}(\cdot)$ are the ϵ -predictions derived from the joint texture-structure model, p_c correspond to the canonical pose map and w_t is the noise sampler.

Prompt Modeling ($\mathbf{P}_{\text{human}}$). To systematically generate diverse descriptions (template) for synthetic data generation, we designed a prompt modeling framework. This framework incorporates a comprehensive set of attributes, including ethnicity, hair type, hair length, hair color, clothing color, clothing patterns, body types, and age groups, to generate realistic and varied character templates as shown in Figure 3. Each attribute was treated as a parameter within

a cyclic iterator, ensuring balanced sampling and avoiding repetitive combinations. The framework dynamically combines these attributes into descriptive sentences (template) tailored to specific scenarios based on the activity.

3.3. Scene Composition

This subsection is organized into the following stages: (1) The canonical human Gaussian is deformed using expert motion sequences; (2) The deformed Gaussians are rasterized from a specified camera viewing direction (ϕ); and (3) A background diffusion algorithm generates the corresponding background for the rasterized Gaussian, guided by a scene prompt ($\mathbf{P}_{\text{scene}}$).

Deformation Module. The generated canonical avatars from Section 3.2 are deformed based on the motion sequences computed from Section 3.1. Given an input motion sequence, each frame provides body pose parameters and a global orientation. These parameters are used to update the mesh vertices to represent the current human pose. Following literature [31, 21] which utilizes the precomputed face associations, barycentric coordinates, and local surface normals, the positions of the Gaussians are recomputed at



Figure 4: **Qualitative examples of synthetic images.** Using **Gen4D**, we applied diverse prompt modeling to generate images across the three sports categories included in the SportPAL dataset.

each frame, ensuring that the deformation of the Gaussian cloud closely follows the articulated motion of the underlying mesh. To maintain fidelity during deformation, points with excessive deviation between the expected and actual projected positions are culled. This filtering ensures stability and avoids visual artifacts due to misalignments during rapid or complex motions.

Rasterization. Once the Gaussians have been deformed according to the target pose, they are rasterized into a 2D image plane. Following standard 3D Gaussian splatting methods [27], each Gaussian is projected using perspective projection based on the camera’s intrinsic and extrinsic parameters. The final image at each pixel is computed by blending Gaussian contributions weighted by opacity and spatial extent, enabling photorealistic rendering without aliasing.

Camera Control. The camera view is dynamically adjusted to capture the deformed model from different viewpoints. Instead of continuously orbiting around the model, the camera position and orientation (elevation and azimuth parameters) are randomly updated for each motion sequence to achieve the desired perspective. The intrinsic parameters, such as field of view, aspect ratio, and near/far

clipping planes, remain fixed.

Background Diffusion. The diffusion module accommodates two tasks: removing artifacts from the rasterized avatars and inducing relevant background in the rasterized human projection. This process results in realistic avatars with scenes as depicted in Figure 4, where the output shows scenes augmented with the rasterized humans.

We utilize IC-Light [55] as the backbone for background generation through its physically grounded light transport consistency principle. This approach ensures that intrinsic object properties, such as albedo and reflectance colors, remain unaltered while accurately modifying illumination effects. This blending of the rasterized avatars with dynamically generated backgrounds results in realistic generated data. The algorithm is driven by an objective function denoted as $\mathcal{L}_{\text{diff}}$ as defined in Equation (2).

$$\mathcal{L}_{\text{diff}} = \lambda_v \left[\|\varepsilon - \delta(\epsilon(I_L)_t, L, t, \epsilon(I_d))\|_2^2 \right] + \lambda_{ic} \left[\|M \odot (\epsilon_{L_1+L_2} - \delta(\epsilon(L_1, L_2)))\|_2^2 \right] \quad (2)$$

where λ_v and λ_{ic} are the weights assigned to 1 and 0.1 by

Table 2: **Performance of 2D HPE techniques across the SportPAL dataset.** The best result is highlighted in **bold** format.

| Method | Baseball | | | Icehockey | | | Soccer | | |
|-----------------|-------------------|--------------------|--------------------|-------------------|--------------------|--------------------|-------------------|--------------------|--------------------|
| | AP ⁵ ↑ | AP ¹⁰ ↑ | AP ¹⁵ ↑ | AP ⁵ ↑ | AP ¹⁰ ↑ | AP ¹⁵ ↑ | AP ⁵ ↑ | AP ¹⁰ ↑ | AP ¹⁵ ↑ |
| DETR-based [12] | 64.33 | 74.61 | 77.19 | 45.01 | 61.7 | 70.46 | 64.85 | 81.04 | 88.20 |
| TokenPose [17] | 80.74 | 89.35 | 93.68 | 62.75 | 96.92 | 99.91 | 67.28 | 92.56 | 98.51 |

default, respectively. M denotes the foreground mask, L_1 and L_2 are the illumination masks, I_L denotes the appearance image, and L represents the environment illumination. ε is the latent representation of an image, δ is the network used to predict noise, ϵ is the diffusion target and I_d represents the degradation image.

The technique involves imposing constraints based on the linearity of light transport, such that the illumination of objects under mixed lighting is consistent with their lighting conditions [16]. This constraint is integrated into the diffusion-based generator, allowing for precise control over foreground and background lighting, including shadow induction for enhanced realism.

4. Dataset

Based on **Gen4D**, we present the largest dataset featuring the most diverse range of actions from various sports, termed as SportPAL, short for Sport Pose and Action Library. This dataset includes activities from three different sports, including baseball, icehockey, and soccer. It provides 2D bounding boxes, groundtruth 2D and 3D human pose annotations, SMPLX human pose and shape parameters, along with the action class. Comprising more than 2,000 videos with 50 subjects representing a wide range of body types and ethnicities, and over 500,000 frames, this dataset offers a rich resource for research on various in-the-wild human-centric vision tasks. Table 3 shows the data split of SportPAL categorized based on the sport.

5. Experiments

5.1. Training Details

The Gaussian model is initialized with 100k samples on the SMPLX mesh with an opacity set to 1. Colors are represented using Spherical Harmonics (SH) coefficients of degree 0. The bidirectional SDS loss weights λ_1 and λ_2 are both set to be 0.5. The training resolution is set to be 1024 with a batch size of 8. The training of the canonical Gaussian is done for 3600 iterations, and it takes about two hours on a single GPU of NVIDIA A6000 (48GB) GPU. The adaptive densifying and pruning is done from 300 to 800 iterations at an interval of 100 steps.

Table 3: **SportPAL Data Split.** Data statistics across three sports collected using the proposed **Gen4D** framework. ‘frames-aug’ denotes total frames after augmentations.

| Sport | Split | #Subjects | #Clips | #Frames |
|--------------|-------|-----------|--------------|----------------|
| Baseball | Train | 15 | 1,000 | 253,869 |
| | Valid | 15 | 304 | 80,810 |
| | Test | 5 | 300 | 71,875 |
| Icehockey | Train | 10 | 195 | 75,468 |
| | Valid | 10 | 50 | 18,867 |
| | Test | 5 | 12 | 7,487 |
| Soccer | Train | 10 | 116 | 57,110 |
| | Valid | 10 | 30 | 14,277 |
| | Test | 5 | 5 | 3,639 |
| Total | - | 50 | 2,012 | 583,403 |

Table 4: **Quantitative comparison of the impact of finetuning on the Icehockey and Soccer datasets.** The best result is highlighted in **bold** format.

| Sport | Method | AP ⁵ ↑ | AP ¹⁰ ↑ | AP ¹⁵ ↑ |
|-----------|----------------|-------------------|--------------------|--------------------|
| Icehockey | w/o finetuning | 62.75 | 96.92 | 99.91 |
| | w/ finetuning | 63.47 | 98.10 | 99.98 |
| | | (+0.72) | (+1.18) | (+0.07) |
| Soccer | w/o finetuning | 67.28 | 92.56 | 98.51 |
| | w/ finetuning | 71.46 | 94.68 | 99.13 |
| | | (+4.18) | (+2.12) | (+0.62) |

Augmentations. We vary the virtual camera parameters for each sequence to capture a wide range of viewing perspectives to improve generalization for arbitrary camera orientations. Specifically, we adjust the azimuth angle (i.e., rotating the camera horizontally around the subject) to simulate different viewpoints.

5.2. Preliminary Results

In this section, we present two pivotal experiments designed to demonstrate the quality of the SportPAL dataset. Specifically, we evaluate the performance of 2D HPE models on the SportPAL dataset—both for training and testing—across the three sports: baseball, ice hockey, and soccer. We assess the efficacy of two different pose estimation architectures and explore the impact of fine-tuning across different sport domains.

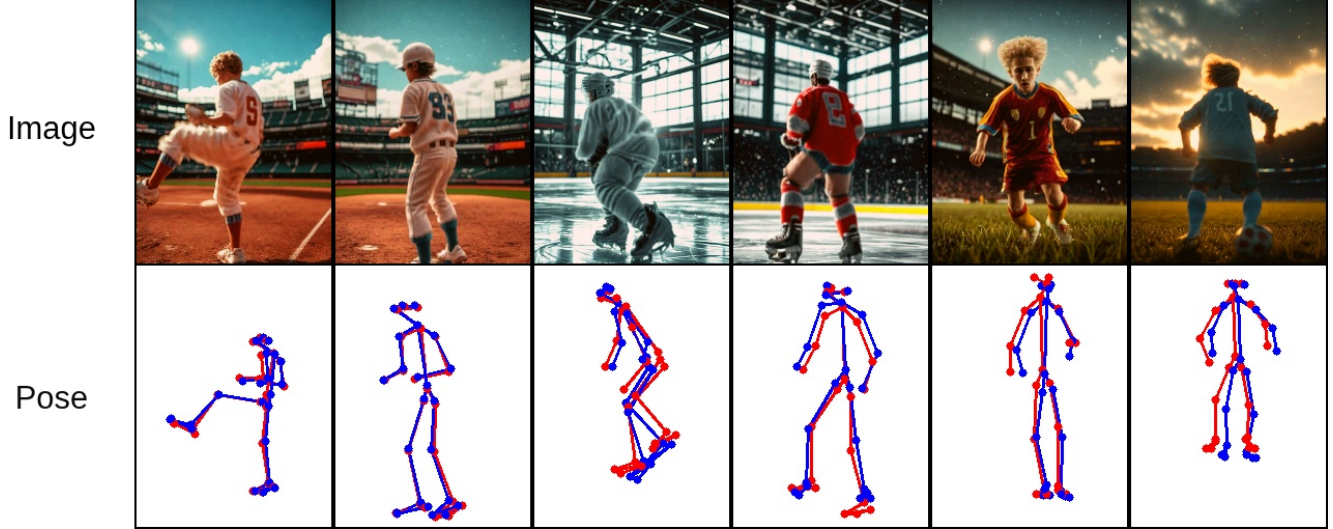


Figure 5: **Qualitative visualizations of pose estimation results generated by TokenPose [29].** Groundtruth and predicted keypoints are shown in **red** and **blue**, respectively.

Pose Estimation Performance on SportPAL. Table 2 summarizes the quantitative results of 2D HPE on the SportPAL dataset for each of the three sports. We trained and evaluated two models: (1) A baseline pose estimator based on a transformer architecture derived from Detection Transformers (DETR) [12]; and (2) the TokenPose model [29], a transformer-based pose estimator designed for dense spatial correspondence learning.

Both models were trained individually on each sport subset of the SportPAL dataset using the same experimental settings for consistency and comparability. As shown in Table 2, TokenPose consistently outperforms the baseline model across all sports, demonstrating superior spatial reasoning and robustness to sport-specific variations in appearance, motion, and occlusion. The improvements are particularly notable in icehockey where the baseline model failed considerably. Some visualization results of TokenPose on test set of the respective sports category are shown in Figure 5.

Cross-Sport Fine-Tuning. To further demonstrate the benefit of data diversity in SportPAL, we conducted a cross-sport fine-tuning experiment, as shown in Table 4. We initially trained the TokenPose model on the baseball subset, which is the largest among the three categories. Subsequently, we fine-tuned this pretrained model separately on the icehockey and soccer subsets, which have comparatively less training data. Compared with directly training on icehockey or soccer data, consistent improvement across both sports was observed after fine-tuning. This result shows that the diversity of our generated data can be benefit for model’s generalizability.

However, the degree of improvement varied. Icehockey

showed marginal gains, likely due to the distribution gap between baseball and icehockey, while notable improvements were observed in soccer. This could be due to the nature of sports, where baseball and soccer involve running-based locomotion, whereas icehockey features skating, which results in significantly different body posture and joint articulation. Additionally, icehockey players usually have bulky gear, occluding the player’s joint positions. Thus, this domain disparity limits the effectiveness of transferring learned representation from baseball to icehockey.

Qualitative Results. Figure 4 illustrates some synthetic images from SportPAL dataset generated using **Gen4D** framework. Some notable aspects include the shadows of the human reflected on the scene, making it more realistic. The illustrations also show varying lighting conditions, camera angles, and varying cloth appearances.

6. Conclusion

In this work, we introduced **Gen4D**, a fully automated and scalable pipeline for generating lifelike 4D human animations with rich diversity across motion, appearance, and environmental conditions, without the need for manual 3D modeling or scene design. Leveraging this framework, we created SportPAL, the largest synthetic dataset for sports-focused, human-centric vision tasks, complete with high-quality annotations across multiple modalities. Our experiments validate the effectiveness of both the dataset and the underlying generation pipeline, demonstrating potential for advancing HPE and related tasks in challenging real-world scenarios where traditional data collection is limited.

Future Work. While **Gen4D** offers a flexible framework for generating diverse and realistic 4D human animations, several promising directions remain for future exploration. First, enforcing temporal consistency across background generation could enable the creation of dynamic, coherent scenes, further supporting downstream video-based applications [54, 13]. Second, optimizing the pseudo groundtruth extracted from expert demonstrations with physics-based constraints could reduce motion jitter and improve the physical plausibility of pose predictions, enhancing the overall realism of generated sequences.

Acknowledgement We sincerely thank the Baltimore Orioles of Major League Baseball for their generous support through the Mitacs Accelerate Program, which was instrumental in advancing this research.

References

- [1] Adobe Systems. Adobe fuse cc. <https://www.adobe.com/es/products/fuse.html>. Accessed: 2025-05-16.
- [2] Adobe Systems. Mixamo: 3d character animation. <https://www.mixamo.com/>. Accessed: 2025-05-16.
- [3] Baves Balaji, Jerrin Bright, Yuhao Chen, Sirisha Rambhatla, John Zelek, and David Clausi. Seeing beyond the crop: Using language priors for out-of-bounding box key-point prediction. *Advances in Neural Information Processing Systems*, 37:102897–102918, 2024.
- [4] German Barquero, Sergio Escalera, and Cristina Palmero. Seamless human motion composition with blended positional encodings. In *Proceedings of the IEEE/CVF Conference on Computer Vision and Pattern Recognition*, pages 457–469, 2024.
- [5] Eduard Gabriel Bazavan, Andrei Zanfir, Mihai Zanfir, William T Freeman, Rahul Sukthankar, and Cristian Sminchisescu. Hspace: Synthetic parametric humans animated in complex environments. *arXiv preprint arXiv:2112.12867*, 2021.
- [6] Michael J Black, Priyanka Patel, Joachim Tesch, and Jinlong Yang. Bedlam: A synthetic dataset of bodies exhibiting detailed lifelike animated motion. In *Proceedings of the IEEE/CVF Conference on Computer Vision and Pattern Recognition*, pages 8726–8737, 2023.
- [7] Blender Foundation. Blender - a 3d modelling and rendering package. <https://www.blender.org/>. Accessed: 2025-05-16.
- [8] Jerrin Bright, Baves Balaji, Harish Prakash, Yuhao Chen, David A Clausi, and John Zelek. Distribution and depth-aware transformers for 3d human mesh recovery. *arXiv preprint arXiv:2403.09063*, 2024.
- [9] Jerrin Bright, Yuhao Chen, and John Zelek. Mitigating motion blur for robust 3d baseball player pose modeling for pitch analysis, 2023.
- [10] Zhongang Cai, Wanqi Yin, Ailing Zeng, Chen Wei, Qingping Sun, Wang Yanjun, Hui En Pang, Haiyi Mei, Mingyuan Zhang, Lei Zhang, Chen Change Loy, Lei Yang, and Ziwei Liu. SMPLer-X: Scaling up expressive human pose and shape estimation. In *Advances in Neural Information Processing Systems*, 2023.
- [11] Zhongang Cai, Mingyuan Zhang, Jiawei Ren, Chen Wei, Daxuan Ren, Zhengyu Lin, Haiyu Zhao, Lei Yang, Chen Change Loy, and Ziwei Liu. Playing for 3d human recovery. *IEEE Transactions on Pattern Analysis and Machine Intelligence*, 2024.
- [12] Nicolas Carion, Francisco Massa, Gabriel Synnaeve, Nicolas Usunier, Alexander Kirillov, and Sergey Zagoruyko. End-to-end object detection with transformers. In *European conference on computer vision*, pages 213–229. Springer, 2020.
- [13] Xingyu Chen, Yue Chen, Yuliang Xiu, Andreas Geiger, and Anpei Chen. Easi3r: Estimating disentangled motion from dust3r without training. *arXiv preprint arXiv:2503.24391*, 2025.
- [14] Subramanian Chidambaram, Rahul Jain, Sai Swarup Reddy, Asim Unmesh, and Karthik Ramani. Annotatexr: An ex-

- tended reality workflow for automating data annotation to support computer vision applications. *Journal of Computing and Information Science in Engineering*, 24(12), 2024.
- [15] Hongsuk Choi, Gyeongsik Moon, and Kyoung Mu Lee. Pose2mesh: Graph convolutional network for 3d human pose and mesh recovery from a 2d human pose. In *Computer Vision–ECCV 2020: 16th European Conference, Glasgow, UK, August 23–28, 2020, Proceedings, Part VII 16*, pages 769–787. Springer, 2020.
 - [16] Paul Debevec, Tim Hawkins, Chris Tchou, Haarm-Pieter Duiker, Westley Sarokin, and Mark Sagar. Acquiring the reflectance field of a human face. In *Proceedings of the 27th annual conference on Computer graphics and interactive techniques*, pages 145–156, 2000.
 - [17] Sai Kumar Dwivedi, Yu Sun, Priyanka Patel, Yao Feng, and Michael J Black. Tokenhmr: Advancing human mesh recovery with a tokenized pose representation. In *Proceedings of the IEEE/CVF Conference on Computer Vision and Pattern Recognition*, pages 1323–1333, 2024.
 - [18] Epic Games. Unreal engine. <https://www.unrealengine.com>, 2020. Accessed: 2025-05-16.
 - [19] Nicola Garau, Giulia Martinelli, Piotr Bródka, Niccolò Bisagno, and Nicola Conci. Panoptop: A framework for generating viewpoint-invariant human pose estimation datasets. In *Proceedings of the IEEE/CVF International Conference on Computer Vision*, pages 234–242, 2021.
 - [20] Liangxiao Hu and Hongwen Zhang. Gaussianavatar: Towards realistic human avatar modeling from a single video via animatable 3d gaussians, 11 2023.
 - [21] Shoukang Hu and Ziwei Liu. Gauhuman: Articulated gaussian splatting from monocular human videos. 2023.
 - [22] Christian Keilstrup Ingwersen, Christian Mikkelsen, Janus Nørtoft Jensen, Morten Rieger Hannemose, and Anders Bjørholm Dahl. Sportspose: A dynamic 3d sports pose dataset. In *Proceedings of the IEEE/CVF International Workshop on Computer Vision in Sports*, 2023.
 - [23] Catalin Ionescu, Dragos Papava, Vlad Olaru, and Cristian Sminchisescu. Human3.6m: Large scale datasets and predictive methods for 3d human sensing in natural environments. *IEEE Transactions on Pattern Analysis and Machine Intelligence*, 36(7):1325–1339, jul 2014.
 - [24] Tianjian Jiang, Johsan Billingham, Sebastian Müksch, Juan Zarate, Nicolas Evans, Martin R Oswald, Marc Pollefeys, Otmar Hilliges, Manuel Kaufmann, and Jie Song. Worldpose: A world cup dataset for global 3d human pose estimation. In *European Conference on Computer Vision*, pages 343–362. Springer, 2024.
 - [25] Sam Johnson and Mark Everingham. Clustered pose and nonlinear appearance models for human pose estimation. In *bmvc*, volume 2, page 5. Aberystwyth, UK, 2010.
 - [26] Angjoo Kanazawa, Michael J Black, David W Jacobs, and Jitendra Malik. End-to-end recovery of human shape and pose. In *Proceedings of the IEEE conference on computer vision and pattern recognition*, pages 7122–7131, 2018.
 - [27] Bernhard Kerbl, Georgios Kopanas, Thomas Leimkuehler, and George Drettakis. 3d gaussian splatting for real-time radiance field rendering. *ACM Trans. Graph.*, 42(4), jul 2023.
 - [28] Ruilong Li, Sha Yang, David A. Ross, and Angjoo Kanazawa. Ai choreographer: Music conditioned 3d dance generation with aist++. *2021 IEEE/CVF International Conference on Computer Vision (ICCV)*, pages 13381–13392, 2021.
 - [29] Yanjie Li, Shoukui Zhang, Zhicheng Wang, Sen Yang, Wankou Yang, Shu-Tao Xia, and Erjin Zhou. Tokenpose: Learning keypoint tokens for human pose estimation. In *Proceedings of the IEEE/CVF International conference on computer vision*, pages 11313–11322, 2021.
 - [30] Tsung-Yi Lin, Michael Maire, Serge Belongie, James Hays, Pietro Perona, Deva Ramanan, Piotr Dollár, and C Lawrence Zitnick. Microsoft coco: Common objects in context. In *Computer Vision–ECCV 2014: 13th European Conference, Zurich, Switzerland, September 6–12, 2014, Proceedings, Part V 13*, pages 740–755. Springer, 2014.
 - [31] Xian Liu, Xiaohang Zhan, Jiaxiang Tang, Ying Shan, Gang Zeng, Dahua Lin, Xihui Liu, and Ziwei Liu. Humangaussian: Text-driven 3d human generation with gaussian splatting. In *Proceedings of the IEEE/CVF Conference on Computer Vision and Pattern Recognition*, pages 6646–6657, 2024.
 - [32] Matthew Loper, Naureen Mahmood, Javier Romero, Gerard Pons-Moll, and Michael J. Black. *SMPL: A Skinned Multi-Person Linear Model*. Association for Computing Machinery, New York, NY, USA, 1 edition, 2023.
 - [33] Naureen Mahmood, Nima Ghorbani, Nikolaus F Troje, Gerard Pons-Moll, and Michael J Black. Amass: Archive of motion capture as surface shapes. In *Proceedings of the IEEE/CVF international conference on computer vision*, pages 5442–5451, 2019.
 - [34] MakeHuman Community. Makehuman: Open source 3d human creator. <http://www.makehumancommunity.org/>. Accessed: 2025-05-16.
 - [35] Dushyant Mehta, Helge Rhodin, Dan Casas, Pascal Fua, Oleksandr Sotnychenko, Weipeng Xu, and Christian Theobalt. Monocular 3d human pose estimation in the wild using improved cnn supervision. In *3D Vision (3DV), 2017 Fifth International Conference on*. IEEE, 2017.
 - [36] Julia Moehrmann and Gunther Heidemann. Efficient annotation of image data sets for computer vision applications. In *Proceedings of the 1st International Workshop on Visual Interfaces for Ground Truth Collection in Computer Vision Applications*, pages 1–6, 2012.
 - [37] Aiden Nibali, Joshua Millward, Zhen He, and Stuart Morgan. ASPset: An outdoor sports pose video dataset with 3D keypoint annotations. *Image and Vision Computing*, page 104196, 2021.
 - [38] Priyanka Patel, Chun-Hao P Huang, Joachim Tesch, David T Hoffmann, Shashank Tripathi, and Michael J Black. Agora: Avatars in geography optimized for regression analysis. In *Proceedings of the IEEE/CVF Conference on Computer Vision and Pattern Recognition*, pages 13468–13478, 2021.
 - [39] Albert Pumarola, Jordi Sanchez-Riera, Gary Choi, Alberto Sanfeliu, and Francesc Moreno-Noguer. 3dpeople: Modeling the geometry of dressed humans. In *Proceedings of the IEEE/CVF international conference on computer vision*, pages 2242–2251, 2019.

- [40] Farheen Qazi, Muhammad Naseem, Sonish Aslam, Zainab Attaria, Muhammad Ali Jan, and Syed Salman Junaid. Anovate: Revolutionizing data annotation with automated labeling technique. *VFAST Transactions on Software Engineering*, 12(2):24–30, 2024.
- [41] Zhiyin Qian, Shaofei Wang, Marko Mihajlovic, Andreas Geiger, and Siyu Tang. 3dgs-avatar: Animatable avatars via deformable 3d gaussian splatting. In *Proceedings of the IEEE/CVF Conference on Computer Vision and Pattern Recognition*, pages 5020–5030, 2024.
- [42] Kathleen M Robinette, Sherri Blackwell, Hein Daanen, Mark Boehmer, and Scott Fleming. Civilian american and european surface anthropometry resource (caesar), final report. volume 1. summary. (*No Title*), 2002.
- [43] Ali Rida Sahili, Najett Neji, and Hedi Tabia. Text-driven motion generation: Overview, challenges and directions, 2025.
- [44] Yonatan Shafir, Guy Tevet, Roy Kapon, and Amit H Bermano. Human motion diffusion as a generative prior. *arXiv preprint arXiv:2303.01418*, 2023.
- [45] Leonid Sigal, Alexandru O Balan, and Michael J Black. Humaneva: Synchronized video and motion capture dataset and baseline algorithm for evaluation of articulated human motion. *International journal of computer vision*, 87(1):4–27, 2010.
- [46] Noah Snavely, Steven M. Seitz, and Richard Szeliski. *Photo Tourism: Exploring Photo Collections in 3D*. Association for Computing Machinery, New York, NY, USA, 1 edition, 2023.
- [47] Guy Tevet, Sigal Raab, Brian Gordon, Yoni Shafir, Daniel Cohen-or, and Amit Haim Bermano. Human motion diffusion model. In *The Eleventh International Conference on Learning Representations*, 2023.
- [48] Matt Trumble, Andrew Gilbert, Charles Malleson, Adrian Hilton, and John Collomosse. Total capture: 3d human pose estimation fusing video and inertial sensors. In *2017 British Machine Vision Conference (BMVC)*, 2017.
- [49] Carnegie Mellon University. Cmu graphics lab motion capture database.
- [50] Gul Varol, Javier Romero, Xavier Martin, Naureen Mahmood, Michael J Black, Ivan Laptev, and Cordelia Schmid. Learning from synthetic humans. In *Proceedings of the IEEE conference on computer vision and pattern recognition*, pages 109–117, 2017.
- [51] Timo Von Marcard, Roberto Henschel, Michael J Black, Bodo Rosenhahn, and Gerard Pons-Moll. Recovering accurate 3d human pose in the wild using imus and a moving camera. In *Proceedings of the European conference on computer vision (ECCV)*, pages 601–617, 2018.
- [52] Hongyi Xu, Eduard Gabriel Bazavan, Andrei Zanfir, William T Freeman, Rahul Sukthankar, and Cristian Sminchisescu. Ghum & ghuml: Generative 3d human shape and articulated pose models. In *Proceedings of the IEEE/CVF Conference on Computer Vision and Pattern Recognition*, pages 6184–6193, 2020.
- [53] Calvin Yeung, Tomohiro Suzuki, Ryota Tanaka, Zhuoer Yin, and Keisuke Fujii. Athletpose3d: A benchmark dataset for 3d human pose estimation and kinematic validation in athletic movements. *arXiv preprint arXiv:2503.07499*, 2025.
- [54] Junyi Zhang, Charles Herrmann, Junhwa Hur, Varun Jampani, Trevor Darrell, Forrester Cole, Deqing Sun, and Ming-Hsuan Yang. Monst3r: A simple approach for estimating geometry in the presence of motion. *arXiv preprint arxiv:2410.03825*, 2024.
- [55] Lvmin Zhang, Anyi Rao, and Maneesh Agrawala. Ic-light github page, 2024.